Structure and Burning Velocity of Premixed, Turbulent Hydrogen-Air - Flames

Ardey
N. JURANEK, F. MAYINGER, G. STRUBE
Lehrstuhl A für Thermodynamik,Technische Universität München,
Arcisstraße 21, 8000 München 2

In the combustion of hydrogen chemical kinetic processes are very fast leading to laminar flame thicknesses of the order of a few tens of micrometers. Therefore the effective turbulent burning velocity is determined by turbulent heat and mass transfer processes rather than chemistry. This paper reports on investigations of the turbulent structure and burning velocity of premixed hydrogen-air flames of lean stoichiometries. For the investigations non-intrusive optical measurement techniques, i. e. Raman-spectroscopy and self fluorescence , have been employed to obtain the data without influencing the combustion process. The parameters investigated were the initial hydrogen concentration, the approaching flow velocity as well as initial temperature.

1. EXPERIMENTAL SET-UP

1.1 BURNER

In a tube burner with a cross section of 20 x 30 mm stationary, atmospheric flames were stabilised behind a metal grid with a hole diameter of 5 mm and a blockage ratio (BR) of 44%. Behind each of the openings of the grid a separate flame developed as can bee seen in Fig. 1.

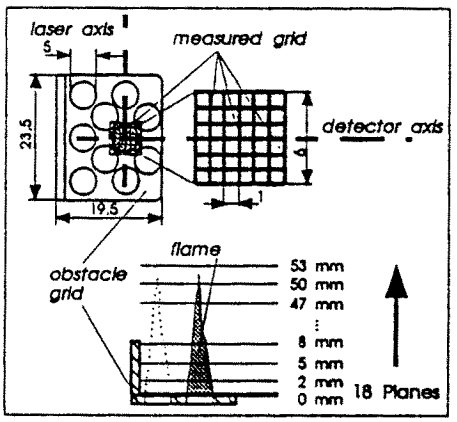

Fig. 1: The flame holder grid configuration

Since the whole burner was uncooled and thermally well isolated and the flames above the openings were surrounded by similar flames, especially the middle flames were effectively shielded from any influence of thermal quenching effects induced from outside the flame. The velocity of the unburned gas approaching the grid was varied from 10 to 20 m/s, corresponding to Reynolds numbers between 10,000 and 20,000 yielding highly turbulent flames. The hydrogen concentrations in the unburned mixtures were varied from 11 vol.% H_2 to 15 vol.% H_2, yielding lean flames with possible quenching effects in the flame front. To study the influence of initial temperature on the flames, the temperature was varied between ambient and 200°C. All together, 17 different flame conditions were investigated.

1.2 Optical measurement techniques

Raman spectroscopy. The main components of the Raman probe employed for the measurements were a pulsed Excimer laser (XeCl) and an intensified diode array detector mounted to the focal exit plane of a spectrograph. Each flame was scanned by Raman measurements (averaged over 75 laser shots) in three dimensions, taking spectra at 49 points in each plane over a total of 18 planes up to a height of 53 mm above the grid (see Fig. 1). Each spectrum was evaluated to obtain the absolute concentrations of the major species H_2 and N_2. As N_2 may be regarded as an inert species, its absolute concentration is inversely proportional to the temperature. Therefore from the obtained data absolute and relative H_2 concentrations as well as the temperature distributions could be evaluated.

Self fluorescence of OH. In addition to the Raman measurements the self fluorescence of OH, the main intermediate species in the hydrogen oxidation, was recorded with an intensified video camera. The main part of natural fluorescence light in H_2-Air flames is emitted by chemiluminiscence, i. e. the OH radicals arise in an electronic excited state and emit light by falling back into their unexcited state (O-O-transition band). Thus reaction zones can be visualised as region of maximal OH emissivity.

2. CLASSIFICATION OF THE FLAMES

The main goal of the investigations concerning this paper was to get a correlation between reaction kinetics, turbulent flow and heat transfer by experimental data leading to a simple burning law. Therefore we have to characterise

the turbulent flow, heat transfer and reaction kinetics in order to get characteristic numbers for ranging the flames into groups.

The simplified conservation laws of mass, energy and impulse without friction effects lead to the following relationships by application of a one dimensional flame front model as described in e. g. [3]. The H_2-air mixture therefore is regarded as an ideal gas. Unburned gases approaching the flame are indicated with index 1 and the burned gases leaving the flame front with index 2:

$$p_1 = p_2 \qquad (1)$$

$$T_2 = T_1(1+Q)\ ;\ Q = \frac{q}{cp\ T_1} \qquad (2)$$

$$\rho_{1/2} = \frac{p}{RT_{1/2}} \qquad (3)$$

$$u_2 = \frac{\rho_1}{\rho_2} u_1 \qquad (4)$$

T_2 is the temperature after the chemical reaction ithout any heat losses and is therefore the adiabatic ourning temperature.

For characterising the burnable gas conditions concerning the chemical reactivity the laminar flame front is a good reference. The most important parameters for turbulent combustion are:

- reaction time τ_c
- laminar burning velocity s_l
- laminar flame thickness δ_l

Since the real temperature in the reaction zone is very closed to the adiabatic burning temperature which is proportional to the initial temperature T_1 Eq. (2) we obtain with the Arrhenius law (e. g. [9] for the reaction time:

$$\tau_c \sim e^{(k_r/T_1)} \qquad (5)$$

With the reaction time the laminar flame thickness may be calculated as following:

$$\delta_l = s_l \tau_c \qquad (6)$$

The correlation between the laminar burning velocity and the reaction time is given by an approximation which can be found e. g. in [13].

$$s_l = \sqrt{\frac{a}{\tau_c}} \qquad (7)$$

With the assumption of $Pr=1$ (an often used simplification in combustion terms (e. g. [9], [2]) we obtain for the laminar burning velocity:

$$\delta_l = \frac{\nu}{s_l} \qquad (8)$$

Generally turbulent flow velocity is modelled as a superposition of the mean velocity $\bar{u}$ and the turbulence intensity u':

$$u(t,x,y,z) = \bar{u}(t,x,y,z) + u'(t,x,y,z) \qquad (9)$$

The corresponding characteristic number is the degree of turbulence.

$$Tu = \frac{u'}{\bar{u}} \qquad (10)$$

With $Tu > 0$ the orthogonal mass transfer leads to a structure with different extended eddies. Turbulent flames are mainly influenced by the eddies largeness and lifetime. The length scale of the eddies can be divided into three classes. The macro scale L (i. e. the diameter of the largest eddy that can be stabilised in the flow) depends on the local geometry and is usually in the dimension of this geometry. Based on a theoretical definition [8] the Taylor micro scale λ_T represents the class of eddies with the highest frequency density. The lowest vorticity that can be regarded as a correlated motion of some molecules is classified by the Kolmogorow microscale l. The relationship between those length scales depending on the energy dissipation ratio ε (eliminated already), the turbulence intensity and the viscosity is given by the following equations [1]:

$$\frac{\lambda_T}{l^2} = \sqrt{15}\frac{u'}{\nu} \qquad (11)$$

$$\frac{l^4}{L} = \frac{k}{15}\frac{\nu^3}{u'^3} \qquad (12)$$

The proportional rate k was detected by Abdel-Gayed et al. [2] as k=40.4 and by Andrews et al. [1] as 48.68. Since no experiments for detecting k were done the value k=48.68 was taken as reference for own calculations.

Describing the influence of the eddies length scale on turbutent flames the following definitions for turbulent Reynolds numbers will be used:

$$\mathrm{Re}_L = \frac{Lu'}{\nu}\ ;\ \mathrm{Re}_\lambda = \frac{\lambda_T u'}{\nu} \qquad (13)$$

Both Reynolds numbers are correlated using Eq. (11)-(12):

$$\mathrm{Re}_{\lambda_T} = \sqrt{k\ \mathrm{Re}_L} \qquad (14)$$

Based on the characteristic length scales the corresponding lifetimes can be calculated. Because of the increasing dissipation ratio ε with increasing turbulence intensity u' life time of macro scale eddies is reciprocally proportional to the turbulence intensity and we obtain the approximation

$$\tau_t = \frac{L}{u'} \qquad (15).$$

Corresponding to the intermolecular forces the time number for Kolmogorow micro scale is given by [11]:

$$\tau_K = \sqrt{\frac{\nu}{\varepsilon}} \qquad (16)$$

Classifying flames concerning the structure is possible with numbers expressing the correlation between reaction kinetics and turbulent flow. Therefore two ratios are taken between the characteristical time numbers:

Damköhler: $Da = \frac{\tau_t}{\tau_c}$ (17)

Karlowitz: $Ka = \frac{\tau_c}{\tau_K} = \left(\frac{\delta_l}{l}\right)^2$ (18)

If the life time of macro scale eddies is longer than the complete reaction of the eddies content takes (i. e. $Da > 1$) the stable regions with burned gases will cause a wrinkled or corrugated flame structure, whereas $Da < 1$ leads to homogeneous reaction zones called *well stirred reactor*. With $Ka>1$ reaction takes less time than the Kolmogorow microscale eddies are alive. Thus reaction zones will be unsharpened and with increasing Ka molecules may be separated before reaction is completed yielding extinguation effects; the corresponding structure is called *distributed reaction zones*. A further criterion for characterising flames is given by the ratio between u' and s_l. If the flame is not able to follow the turbulent flow in the view of an eddy fixed co-ordinate system (i. e. $u'/s_l > 1$) flame regions may breakaway leading to a corrugated flame structure. The whole region representing $Ka<1$ is called *flamelet regime* characterising flames with a thickness smaller than any eddy. The behaviour of the flame front itself is similar to laminar flame fronts which propagate orthogonal to their extention any time. The joining line between burned and unburned gases crosses a reaction zone at any place and any time, i. e. unburned gases must be surrounded by a closed flame front any time.

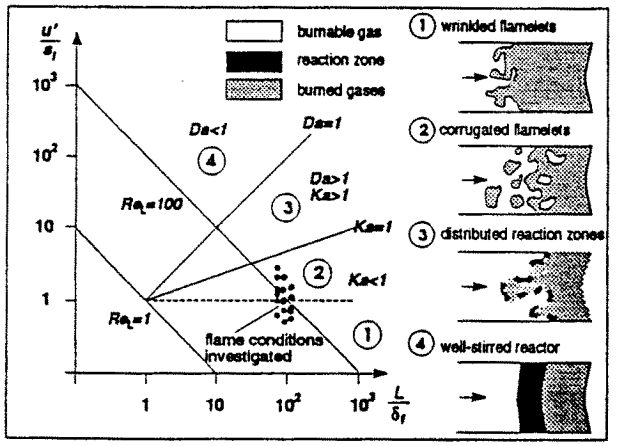

Fig. 2: Phase plot after Borghi [5]

Because no LDA-measurements of the investigated burner are available yet a careful comparison to the literature was taken [7], [10], [6] in order to get some reference values for the degree of turbulence Tu for this special arrangement. According to Andrews et al. [1] Tu may be considered as approximately constant and was estimated as Tu=0.07. Since only those eddies which are smaller than the hole diameter of the flame holder grid are able to pass it the macro scale L was taken to be 4 mm long according to a contraction ratio of 0.65 [12]. Knowing Tu, L and s_l all necessary data for characterising the flame structure can be evaluated with Eq. (1)-(18). To give an overview of the investigated flames it is convenient outlining the flame conditions in a phase plot after Borghi [5] which allows the classification of the flame structure as described above (see Fig. 2).

3. RESULTS

3.1 Flame contour

Raman measurements After evaluation of all Raman spectra the H_2 - relative concentration profiles were available for every plane in steps of 2 mm for the middle flame cone over the grid for any varied parameter (see Fig. 1 and Fig. 3). Obviously there is a maximum concentration of H_2 over the middle of the hole whereas the concentration decreases dramatically reaching the hole margin indicating the reaction zone. The peaks that can be seen at the profile edges belong to the adjacent flames (see. Fig. 3). The H_2 concentration also decreases by increasing height of the taken profile over the grid leading to the conclusion that the outer contour of the flame is conic as expected.

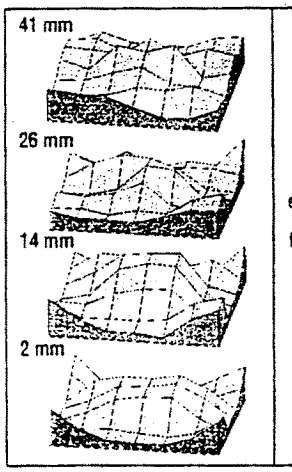

Fig. 3: H_2-concentration profiles over the grid

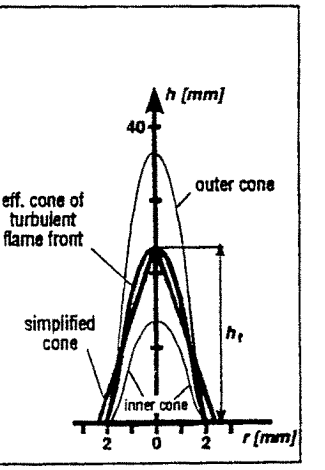

Fig.4: The turbulent flame cones

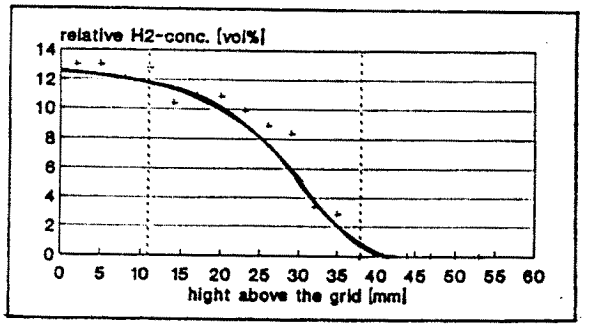

Fig. 5: Relative H_2-concentration over the vertical axis

Fig. 5 shows the H_2 concentration march over the vertical axis for a flame with 100 °C initial temperature, 13 vol.% initial H_2 concentration and an approaching velocity of 10 m/s. Obviously three zones can be distinguished. The

first region is identified by a nearly unchanged H_2 concentration whereas the H_2 concentration decreases in the second region indicating the zone where the reaction takes place until the H_2 disappears completely in the third region. Generally this course could be found under any condition investigated. Therefore the conclusion was: - each flame consisted of three distinct zones (see Fig. 4): an inner cone within which (almost) no reaction takes place and which is enveloped by an outer cone. Between these to cones the wrinkled flame front fluctuates with the turbulent structure of the approaching flow, outside the cone only burned gases are present.

2 mm above the grid hole both the inner and outer cone had the fixed position r=1.6 mm and r=2.0 mm due to the contraction ratio of 0.65. The top of the flame cone fluctuated with the turbulent flow. Whereas the inner cone always was quiet marked the outer cone sharpness decreased with increasing mean flow velocity which could be deduced from an increasing spreading of the results. The reason is an increasing turbulence intensity u' that makes the flame front breaking away yielding corrugated flamelets.

With $u'/s_l < 1$ a correlation could be found between ıe macro scale L and the height of the outer cone just by calculating the maximum height unburned H_2 can reach due to the laminar burning velocity s_l and the macro scale life time τ_t:

$$h_{max} \approx \bar{u}_m \frac{L}{k_h s_l} \qquad (19)$$

The mean velocity $\bar{u}_m$ may be obtained with Eq.(2)-(4):

$$\bar{u}_m \approx \frac{u_1 + u_2}{2} \qquad (20)$$

$$\bar{u}_m = \frac{1}{4}\bar{u}\left(Q(\phi, T_1) + 2\right) \qquad (21)$$

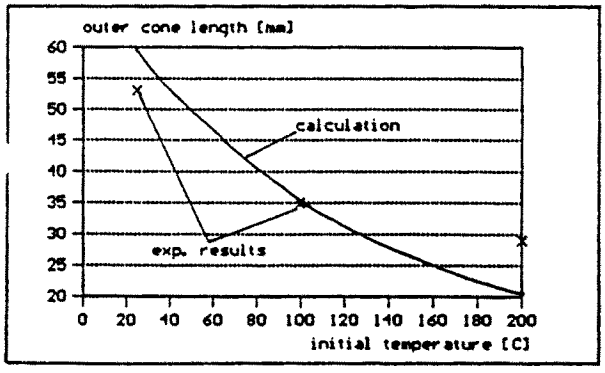

Fig.6: Correlation between the macro scale L and the outer cone length

The condition $u'/s_l < 1$ was given for all flames with an approaching flow velocity of 10 m/s except of the flame with 11 vol.% H_2 and ambient temperature as initial conditions. The proportional rate k_h was found as 1,3 for the best approximation of the experimental data. Fig 6 shows a comparison between the calculated h_{max} and the measured length of the outer cone h_e for e. g. 13 vol.% H_2, an approaching speed of 10 m/s and a temperature of 100 °C as initial conditions. Since the macro scale eddies passing the grid holes will be enlarged by expansion caused by the combustion above the grid the measured decay of the cone length with increasing temperature is less than the calculated decay.

Self fluorescence measurements In order to verify the obtained data self fluorescence measurements were done complementary to the Raman measurements. Since a simultaneous measurement of the whole flame cone is not possible at the test facility only the region up to a height of 15 mm was investigated. How to verify the Raman data will be demonstrated at the initial conditions of 13 vol.% H_2, an approaching speed of 10 m/s and a temperature of 100 °C representing quiet stable burning conditions.

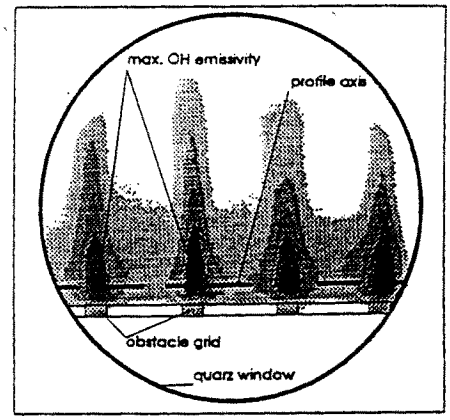

Fig. 7: Self fluorescence image of the flames

In Fig. 7 an image of the self fluorescence can be seen. The darker the image the higher is the OH emissivity as the original recording was monitored in false colours. What can be seen is an integral picture of the fluorescence light from all flame cones. To compare the flame profile obtained by Raman data with the self fluorescence results an Abel transformation has to be applied on the Raman profile taking all flame cones to be rotationally symmetric. Afterwards the integrated profile has to be overlaid due to the grid configuration. This will be done exemplary for the plane 2 mm above the grid.

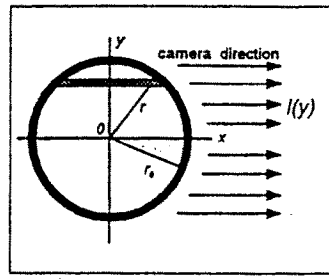

Fig. 8: Abel transformation (scheme)

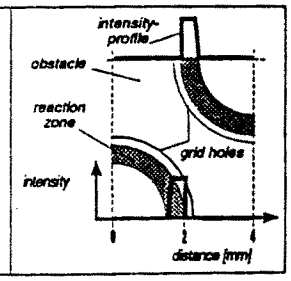

Fig. 9: Overlaying the intensity profiles

With $I(y)$ as the integrated profile and $ER(r)$ as the emissivity profile depending on the radius only the Abel transformation and its inversion is given by the following equations [4] (see Fig. 8):

$$I(y) = 2\int_0^{\sqrt{r_a^2 - y^2}} ER(r)\, dx$$
$$ER(r) = -\frac{1}{\pi}\int_r^{r_a} \frac{\partial I(y)/\partial y}{\sqrt{y^2 - r^2}}\, dy \qquad (22)$$

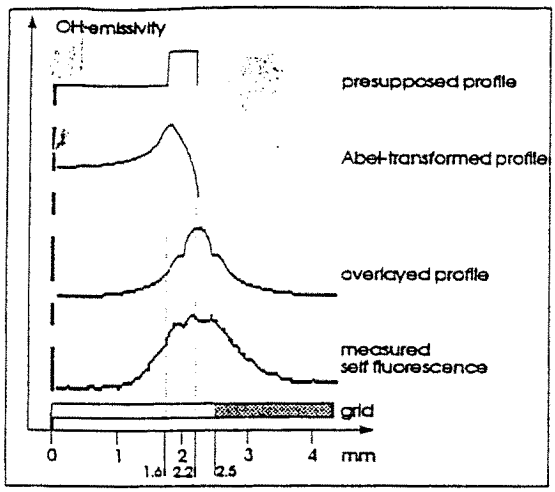

Fig 10: Applying an Abel transformation to compare Raman spectroscopy results with self fluorescence measurements

For a very first approximation the emissivity profile in the reaction zone between the inner and outer cone is taken to be homogeneous. For numerical reasons the discontinuity at the inner cone boundary was changed to a short steady ramp (see Fig. 9). Because of the grids symmetric configuration only two profiles have to be overlaid as can be seen in Fig. 9. A comparison between the calculated and the measured profile matches is displayed in Fig. 10. To get the best accordance the measured outer cone radius obtained by Raman data had to be enlarged from 2 to 2,2 mm. Regarding to a measurement accuracy gained by 2 - 3 mm focal length of the laser beam this may be acceptable.

The unsharpness of the measured self fluorescence profile in compare to the calculated profile may be caused by a less process tolerance of the grid concerning the exact position of the holes.

3.2 Developing a simplified burning law

Knowing the flame structure under the varied conditions it is possible to evaluate a simplified burning law aiming the prediction of the turbulent burning speed in order to translate the results to other similar conditions.

To get the effective turbulent burning velocity s_t the measured integral burning velocity given by the approaching flow velocity $\bar{u}$ it has to be related to the surface area moulded by the flame front:

$$s_t = \frac{u A_d}{(1-BR)} \frac{1}{A_t} \qquad (23)$$

with A_t as surface area of the effective turbulent flame cone, A_d as area of the grid hole and BR as blockage ratio. The effective cone height was found by taking the plane where H_2 concentration decreased to 50% of the initial concentration indicating the place with a maximum probability of the flame front appearing. Thus the effective cone surface A_t may be calculated as follows (see. Fig. 4):

$$A_t = \frac{1}{2}\pi d_t h_t \qquad (24)$$

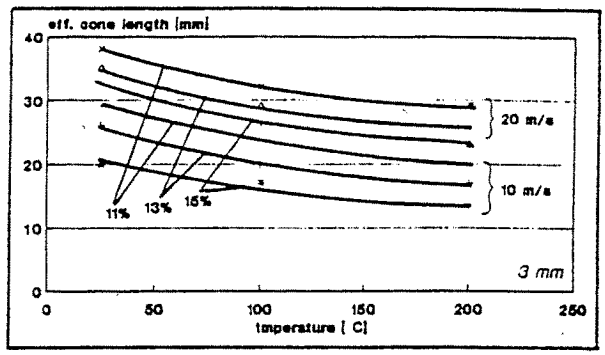

Fig. 11: Effective turbulent flame cone length

The cone basis diameter d_t was taken as 4.5 mm for any flame cone. Taking the investigated parameters the turbulent burning velocity is given by the relation

$$s_t = 5\bar{u}\frac{1}{h_t} \qquad (25)$$

In Fig. 11 the effective cone length under the varied conditions are plotted. Investigating the influence of the different parameters on the cone length by curve fitting techniques make the following proportionalities obviously under consideration of the quiet small parameter regime:

$$h_t \sim \frac{1}{\phi}; \quad h_t \sim \sqrt{\bar{u}}; \quad h_t \sim e^{(k_t/T_1)}; \quad (26)$$

Due to the increasing laminar burning velocity with an increasing equivalence ratio the laminar burning velocity s_l should be taken instead of the equivalence ratio presupposing a linear relationship between s_l and ϕ under the regard of the small parameter field. The exponential expression reflects the main influence of initial temperature due to the Arrhenius law which is applied to Eq. (5). As a well accepted approximation the Prandtl number may be estimated as

$$\mathrm{Pr} = \frac{\nu}{a} \approx 1,0 \qquad (27).$$

Therefore the exponential expression can be eliminated by using Eq. (5)-(8):

$$h_t = e^{(Cx_t/\Pi_1)} = \tau_e^C = \left(\frac{\nu}{s_l^2}\right)^C \qquad (28)$$

The best approximation could be found with C=0,5 which leads to a inversely proportionality to the laminar burning velocity s_l again. Put into Eq. (25) the proportionalities (Eq. (26)-(27)) lead to the following relationship for the turbulent burning velocity:

$$s_t \sim s_l \sqrt{\frac{\overline{u}}{\nu}} \qquad (29)$$

As a very first approach the degree of turbulence Tu was taken to be constant [1] which leads to

$$s_t \sim s_l \sqrt{\frac{u'}{\nu}} \qquad (30).$$

Since the turbulent burning velocity should be identically with the laminar burning velocity under laminar conditions (i. e. Tu=0) the complete approximation is given by

$$s_t = s_l \left(1 + K\sqrt{\frac{u'}{\nu}}\right) \qquad (31)$$

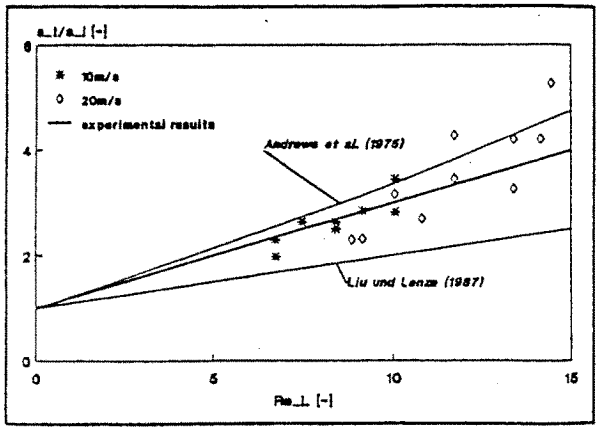

Fig. 12: The turbulent burning velocity obtained by own measurements and modelling in comparison to results taken from the literature [1] u. [9]

The best results according to the experimental data was obtained with K=0.2. All measurements were done with the same flame holder grid. Thus the macro scale L was not varied and the influence of the macro scale on the turbulent burning velocity could not be obtained by the experiments. Therefore a comparison to the literature was taken with the proportionality to the square root of the macro scale according to [1] and [10] as result. The complete approximation for the turbulent burning velocity within the given parameter field is given by:

$$s_t = s_l\left(1 + 0{,}2\sqrt{\mathrm{Re}_L}\right) \qquad (32)$$

In Fig. 12 the turbulent burning velocity related to the laminar burning velocity is plotted over the turbulent Reynolds number Re_L and compared to the literature results [1], [10]. To transform the turbulent Reynolds number Re_λ into the macro scale related Reynolds number Re_L the proportional rate of 48.68 [1] was used. Fig. 12 shows a good agreement between the experimental data and the literature results.

NOMENCLATURE

a	heat transfer coefficient	q	spec. heat flow $q = \dot{Q}/\dot{m}_B$
A_d	area of a grid hole	r	radius
A_t	surface area of flame cones	R	spec. gas constant
e	Euler number	ρ	density
$\dot{m}_B$	mass flow of burnable gas	T	temperature
p	pressure	u	velocity
$\dot{Q}$	heat flow	ν	kin. viscosity
		ϕ	equivalence ratio

REFERENCES

[1] **Andrews G. E., Bradley D., Lwakabamba S. B.**, 1975, Turbulence and Turbulent Flame Propagation - A Critical Appraisal, Comb. and Flame, Vol. 24

[2] **Abdel-Gayed R. G., Bradley D., Lung F. K.-K.**, 1989, Combustion Regimes and the Straining of Turbulent Premixed Flames, Comb. and Flame, Vol. 76

[3] **Bartlmä F.**, 1975 Gasdynamik der Verbrennung, Springer Verlag, Berlin

[4] **Bekefi G.**, 1976, Principles of Laser Plasmas, John Wiley & Sons, New York

[5] **Borghi R.**, On the Structure of Turbulent Premixed Flames; Recent Advances in Aeronautical Science, Eds.: C. Bruno, C. Casci, Pergamon Press

[6] **Cheng R. K., Shepherd I. G.**, 1991, The Influence of Burner Geometry on Premixed Turbulent Flame Propagation, Comb. and Flame, Vol. 85

[7] **Gökalp I., Shepherd I. G., Cheng R. K.**, 1988, Spectral Behaviour of Velocity Fluctuations in Premixed Turbulent Flames, Comb. and Flame, Vol. 71

[8] **Hartmann V.**, 1983, Geschwindigkeits- und Turbulenzmessungen in eingeschlossenen Diffusionsflammen mit Hilfe der Laser-Doppler-Anemometrie, doctoral thesis, TU Stuttgart

[9] **Kuo K. K.**, 1986, Principles of combustion, John Wiley & Sons, New York

[10] **Liu Y., Lenze B.**, 1987, Einflüsse der Frischgemisch-Turbulenzparameter auf die Flammengeschwindigkeit in turbulenten Vormischflammen, 3. TECFLAM-Seminar, Karlsruhe

[11] **Peters N.**, 1986, Laminar Flamelet Concepts in Turbulent Combustion, 21st Symp. (Intl.) on Combustion, The Combustion Institute, Pittsburgh

[12] **Truckenbrodt E.**, 1980, Fluidmechanik, Band 1, Springer Verlag, Heidelberg

[13] **Warnatz J.**, 1981, Concentration-, Pressure-, and Temperature - Dependence of the Flame Velocity in Hydrogen-Oxygen-Nitrogen Mixtures, Combustion Science and Technology, Vol. 26